Modelling iron-powder inductors at high frequenciesProceedings of 1994 IEEE Industry Applications Society Annual Meeting

MODELING IRON-POWDER INDUCTORS AT HIGH FREQUENCIES

M. Bartoli, A. Reatti, Member, IEEE
University of Florence,
Department of Electronic Engineering
Via di S. Marta, 3, 50139 Florence, Italy
Phone: (39)(55)4796-389 and Fax: (39)(55)494569
E - Mail: CIRCUITI@VM.IDG.CNR.FI

M. K. Kazimierczuk, Senior Member, IEEE
Wright State University,
Department of Electrical Engineering
Dayton, Ohio 45435
Phone: (513)873-5059 and Fax: (513)873-5009
E - Mail: MKAZIM@VALHALLA.CS.WRIGHT.EDU

Abstract - **A high-frequency model of iron-powder core inductors is studied. The skin and proximity effects that cause the winding parasitic resistance to increase with the operating frequency are considered. The inductor self-resonance due to the parasitic capacitances is taken into account as well. The frequency response of the inductor model is compared to that of an experimentally tested iron-powder core inductor. The first self-resonant frequency is determined from the plot of the measured reactance and allows for the calculation of the parasitic capacitance. Equations for the inductor parasitic resistance are derived in a closed form. Expressions giving the ac resistance as a function of the operating frequency are given. These expressions allow for an accurate prediction of the inductor power loss over a wide frequency range. The measured and calculated values of the inductor impedance magnitude and phase, the real and imaginary parts of the inductor impedance, the inductance, and the inductor quality factor are plotted versus frequency and compared. Theoretical results were in good agreement with those experimentally measured. Therefore, it is demonstrated that the discussed equivalent circuit has a frequency response matching that of the real inductor. Moreover, the circuit model is simple, it allows for an immediate understanding of iron-powder core inductor behavior and can be easily used in computer simulations of electronic circuits.**

I. INTRODUCTION

The increasing demand for power supplies with small volumes and weights has necessitated the development of switching power converters operating at frequencies above several hundred kilohertz to achieve a size reduction of magnetic components. At high operating frequencies parasitic resistances and capacitances of inductors can adversely affect the operation of power converters. Therefore, an accurate prediction of the frequency response of inductors is crucial to the design of high-frequency power circuits. Parasitic resistance due to core losses is drastically reduced if distributed air gap cores with a low permeability such as iron-powder cores are used. However, the winding ac resistance at high frequencies is much higher than the dc resistance because of the skin and proximity effects. Moreover, many turns must be wound on a low permeability core, resulting in a relatively large parasitic capacitance that affects the inductor frequency response. As a result, the first self-resonant frequency of the inductor is low and parasitic resistance is high at frequencies close to the self-resonant frequency, and the inductor behaves like a capacitor if it is operated above the self-resonant frequency. Unfortunately, the parasitic capacitances and resistances are distributed parameters and their values depend on the operating frequency. Therefore, it is very difficult to theoretically predict the frequency response of an inductor.

The problem of high-frequency magnetic components is discussed in [1]-[13]. In [1], only the skin and proximity effect contributions to the ac resistance are considered. References [2]-[3] deal with the problem of high-frequency transformer and inductor design but do not give any model of these components. Equivalent circuits of magnetic components are shown in references [6] and [7], but the effect of parasitic capacitances on the frequency response is studied in detail for wide-band transformers used in transmission of information. Therefore, the results of these studies cannot be transferred to power magnetic components. High-frequency equivalent circuits of power inductors are given in [8]-[13], but resistances of the models are assumed to be frequency independent and have too low values at high operating frequencies.

The purpose of this paper is to study a circuit model of iron powder-core inductors including both parasitic capacitances and frequency-dependent winding and core resistances. The impedance magnitude and phase, equivalent series resistance R_s (ESR) and reactance X_s, inductance, and quality factor of the equivalent inductor model are plotted as functions of the operating frequency and compared with those obtained experimentally for an iron-powder core inductor. Theoretical and experimental results were in good agreement.

The new contribution of this work is the simple lumped-parameter equivalent circuit that accurately describes the frequency response of iron-powder inductors. A procedure for determining the values the model components is also presented in the paper. The significance of the paper is that the introduced equivalent circuit is simple, leads to a straightforward understanding of the behavior of iron-powder core inductors, and describes their frequency response very accurately. For this reason, it can be usefully used in designing electronic circuits such as EMI filters, resonant circuits, filters for power converters, etc. The inductor operation over a wide range of frequencies can be predicted by using the model. From this examination,

[1] This work was supported by *MagneTek S.p.A.*

0-7803-1993-1/94 $4.00 © 1994 IEEE

operation at frequencies too close to the self-resonant frequency and with too low efficiencies can be prevented. Moreover, the model is particularly suitable for applications in computer simulations of electronic circuits.

II. Inductor Equivalent Circuit And Computational Procedure Of Equivalent Circuit Parameters

A. Equivalent Circuit of Iron-Powder Inductors

Fig. 1 shows an equivalent circuit of a two-layer inductor. Parasitic capacitances affecting the high-frequency inductor operation are the turn-to-turn capacitances of each j-th turn $c_{t\text{-}tj}$, the turn-to-core capacitances $c_{t\text{-}cj}$, and the layer-to-layer capacitances $c_{l\text{-}lj}$. Parasitic resistances are the winding resistance r_j, the core resistance r_{cj} associated with the finite resistivity of the inductor core, and the resistance of the dielectric material coated on the wire r_{dj}. Since the distributed-parameter equivalent circuit of Fig. 1 is cumbersome, a lumped-parameter equivalent circuit of Fig. 2(a) is considered to model the inductor. Here, L is the coil inductance, R_w is the winding resistance, and R_c is the core resistance. Both resistances are frequency dependent. In an inductor wound on an iron-powder core, the turn-to-turn and layer-to-layer capacitances represent the major components of the total parallel capacitance C, shown in Fig. 2(a). The total parasitic ac resistance $R_{ac} = R_w + R_c$ is the series combination of R_w and R_c, as shown in Fig. 2(b).

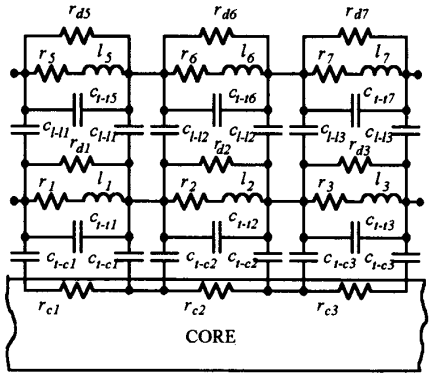

Fig. 1. Model of a two-layer inductor.

The impedance of the equivalent circuits depicted in Figs. 2(a) and (b) is

$$Z_s = \frac{R_{ac} + j\omega L\left(1-\omega^2 LC - CR_{ac}^2/L\right)}{\left(1-\omega^2 LC\right)^2 + \omega^2 C^2 R_{ac}^2} = R_s + jX_s = |Z_s|e^{j\phi} \tag{1}$$

where R_s and X_s are the real and the imaginary parts of Z_s, and $|Z_s|$ and f are the magnitude and phase of Z_s, respectively.

By definition, the self-resonant frequency $f_r = \omega_r/2\pi$ occurs when $X_s = 0$. Since $CR_{ac}^2/L << 1$, (1) gives the inductor parasitic capacitance

$$C = \frac{1}{\omega_r^2 L} = \frac{1}{(2\pi f_r)^2 L}. \tag{2}$$

Fig. 2(c) shows the resistance R_s and reactance X_s measured by LCR meters when the equivalent series circuit model is selected for the device test. Other impedance parameters are calculated by the LCR meters [12] from $R_s + jX_s$. In particular, the equivalent series inductance (ESL) at a given frequency is

$$L_s = \frac{X_s}{\omega}. \tag{3}$$

Since the series equivalent reactance is positive for $f < f_r$ and negative for $f > f_r$, the series inductance L_s becomes negative for frequencies above the self-resonant frequency.

The inductor quality factor at a given frequency is

$$Q_s = \frac{|X_s|}{R_s}. \tag{4}$$

The quality factor can also be defined by using the energy stored in the magnetic field

$$Q_o = 2\pi f \frac{E_L}{P_R} = \frac{\omega L}{R_{ac}} \tag{5}$$

where E_L is the maximum energy stored in the inductor and P_R is the power loss in R_{ac}.

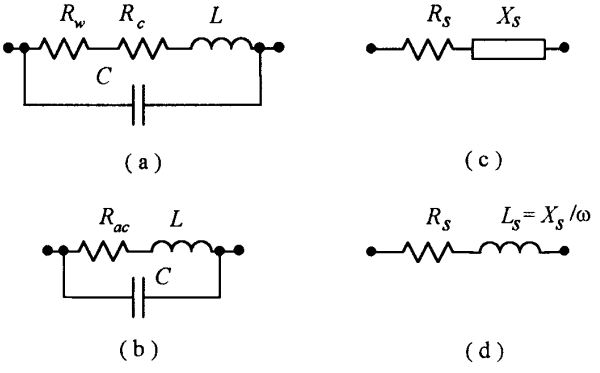

Fig. 2. Equivalent circuits of an inductor.
(a) Lumped parameter equivalent circuit.
(b) Simplified lumped parameter equivalent circuit.
(c) Equivalent series circuit.
(d) Equivalent circuit assumed by many LCR meters.

B. Winding Equivalent Resistance

The winding dc resistance is expressed by

$$R_{dc} = r_L N l_T = \frac{4\rho}{\pi d^2} N l_T \tag{6}$$

where N is the number of turns of the winding, l_T (mm) is the average length of one turn of the winding, r_L (Ω/mm) is the resistance per unit length of the winding wire at a given operating temperature T, d is the conductor diameter in mm, and ρ is the conductor resistivity ($\rho = 17.24x10^{-6}$ Ωmm for a copper conductor at an operating temperature of 20 °C). Wire data sheets usually give two values of r_L at 20 °C and 100 °C; the latter is typically 1.33 times higher than the former.

The ac resistance of a coil winding with an integer number of layers N_ℓ is given by [1]

$$R_w = R_{dc}Re\left\{\frac{A+jA}{tanh(A+jA)}+\frac{2\left(N_\ell^2-1\right)}{3}(A+jA)tanh\left(\frac{A+jA}{2}\right)\right\}$$
$$= R_{dc}A\left\{\frac{e^{2A}-e^{-2A}+2sin2A}{e^{2A}+e^{-2A}-2cos2A}+\frac{2\left(N_\ell^2-1\right)}{3}\frac{e^{A}-e^{-A}-2sinA}{e^{A}+e^{-A}+2cosA}\right\} \quad (7)$$

where [13]

$$A=\left(\frac{\pi}{4}\right)^{3/4}d^{3/2}\left(\frac{\mu_{rw}\mu_o\pi f}{\rho t}\right)^{1/2}=\left(\frac{\pi}{4}\right)^{3/4}\frac{d^{3/2}}{\delta t^{1/2}} \quad (8)$$

f is the operating frequency in hertz, t is the distance between the centres of two adjacent conductors in mm, μ_{rw} is the relative magnetic permeability of the conductor material ($\mu_{rw} = 1$ for a copper conductor), $\mu_o = 4\pi10^{-7}$ H/m $= 4\pi10^{-10}$ H/mm, and the skin depth in mm is

$$\delta=\left(\frac{\rho}{\mu_{rw}\mu_o\pi f}\right)^{1/2}. \quad (9)$$

Fig. 3 shows a plot of the winding ac resistance R_w calculated for a one layer inductor that is made of 95 turns of a solid copper round wire with a diameter $d = 0.45$ mm and is wound on an Amidon T94 toroidal core made of the iron-powder material #2.

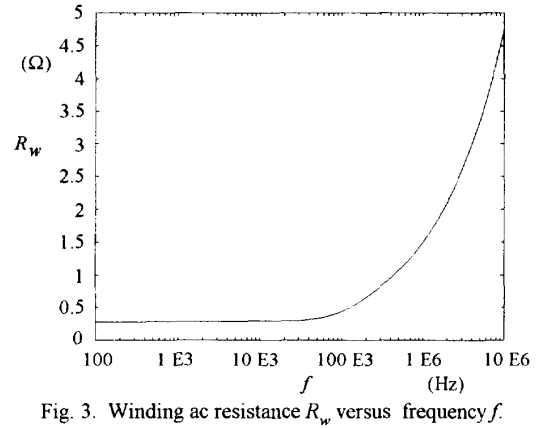

Fig. 3. Winding ac resistance R_w versus frequency f.

The distance between two adjacent turn centers $t = 0.51$ mm is equal to the external diameter of the round wire including the insulation layer. Since the average length of one turn is $l_T = 28$ mm and the resistance of a 0.45 mm diameter wire is $r_L = 106.2x10^{-6}$ Ω/mm at 20 °C, a dc resistance $R_{dc} = 0.28$ Ω is evaluated by using (6). It can be seen from Fig. 3 that the winding resistance is approximately equal to the dc resistance $R_{dc} = 0.28$ Ω up to 40 kHz and then abruptly increases with frequency. It becomes 5 times higher than R_{dc} at $f = 1$ MHz and 15 times higher than R_{dc} at $f = 10$ MHz.

From (7), it follows that a multilayer winding results in a higher ac resistance because the second term of (7) is not zero for $N_l > 1$.

It is shown in the Appendix that the winding ac resistance can be approximated by

$$R_w \approx R_{dc}A\left[1+\frac{2\left(N_\ell^2-1\right)}{3}\right]$$
$$=\left(\frac{4}{\pi}\right)^{1/4}Nl_T\left(\frac{\rho\mu_{rw}\mu_o\pi f}{dt}\right)^{1/2}\left[1+\frac{2\left(N_\ell^2-1\right)}{3}\right] \quad (10)$$

for

$$f \ge f_{bs} = \frac{\rho t}{\mu_{rw}\mu_o\pi d^3}\left(\frac{4}{\pi}\right)^{3/2} \quad \text{if } N_\ell = 1 \quad (11)$$

and for

$$f \ge f'_{bm} = \frac{16\rho t}{\mu_{rw}\mu_o\pi d^3}\left(\frac{4}{\pi}\right)^{3/2} \quad \text{if } N_\ell > 1. \quad (12)$$

Moreover, $R_{ac} \approx R_{dc}$ for $f < f_{bs}$ and for

$$f \le f''_{bm} = \frac{\rho t N_\ell}{N_\ell^3\mu_{rw}\mu_o\pi d^3}\left(\frac{4}{\pi}\right)^{3/2} = \frac{f_{bs}}{N_\ell^2} \quad \text{if } N_\ell = 1. \quad (13)$$

if $N_\ell > 1$. A single layer and a multilayer windings have the same dc resistance if the same diameter wire is wound and the distance between two adjacent turns is increased proportionally to the number of layers. For a solid wire with $d = 0.45$ mm, $t = 0.51$ mm, and $N_\ell = 1$, (11) gives $f_{bs} = 35$ kHz. From (7), the winding ac resistance is $R_w = 1.07R_{dc}$ at $f = 35$ kHz.

Fig. 4 depicts plots of the exact and approximated ac resistances calculated from (7) and (13), respectively, for the winding with $N_\ell = 2$, $d = 0.45$ mm, and $t = 1.02$ mm. Observe that both plots become identical for $f > 0.8$ MHz which is consistent with inequality (12). From (13), we have $f''_{bm} = 8.75$ kHz. At this frequency, the ac resistance for a two layer winding with $d = 0.45$ mm and $t_{Nl} = 1.02$ mm resulting from (7) is $R_w = 1.07\,R_{dc}$.

Comparison of Figs. 3 and 4 shows that the same wire wound on two layers has an ac resistance higher than when it is wound on one layer only. This yields the following

design rule: once the number of turns on the winding is known, the wire should have the largest diameter which still allows the winding to fit in one layer.

C. Core Equivalent Resistance

Power losses occurring in magnetic materials are: hysteresis losses, residual losses, and eddy current losses. Power loss due to the hysteresis and residual losses can be specified per unit volume, while eddy current loss not only depends on the core volume but also on its shape. For this reason, eddy current losses should be separately calculated. Since the eddy currents for relatively small toroidal cores have very small amplitude, the contribution of eddy current loss to the core resistance R_c is neglected (this is in agreement with recommendations of Standard IEC 401).

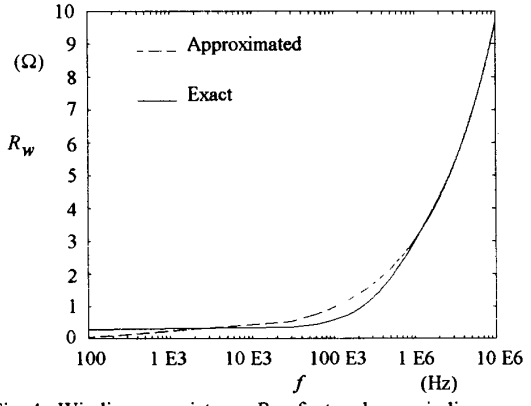

Fig. 4. Winding ac resistance R_w of a two layer winding versus frequency f.

The core loss per unit volume is given by

$$P_{CV} = Kf^x B_m^y \tag{14}$$

were P_{CV} is given in W/m^3 and x, y, and K are coefficients, dependent on the core material. Coefficient K also depends on the inductor operating temperature. The maximum ac flux density the core is operated at is expressed as

$$B_m = \mu_{rc}\frac{\mu_o N I_m}{l_e} = \frac{L I_m}{N A_e}\ (T) \tag{15}$$

where I_m (A) is the amplitude of the current through R_c, μ_{rc} is the core relative magnetic permeability, l_e (m) is the length of the core magnetic path, and A_e is the core cross sectional area (m^2) . The power loss in core resistance R_c of Fig. 2(a) is

$$P_{RC} = V_e P_{CV} = \frac{1}{2} R_c I_m^2\ (W) \tag{16}$$

where V_e is the core volume (m^3). Combination of (14) through (16) yields the core resistance

$$R_c = 2Kf^z\left(\mu_{rc}\frac{\mu_o N}{l_e}\right)^y I_m^{y-2} V_e = 2Kf^z\left(\frac{L}{NA_e}\right)^y I_m^{y-2} V_e \tag{17}$$

For a Amidon material #2 T--94 toroidal core, μ_{rc} = 10, $K = 8.87 \times 10^{-7}$ at 20 °C, x = 1.14, y = 2.19, $l_e = 6 \times 10^{-2}$ m, $A_e = 38.5 \times 10^{-6}$ m^2, and $V_e = 2.31 \times 10^{-6}$ m^3. Resistance R_c calculated at flux densities of 45 and 250 mT is plotted versus frequency in Fig. 5. Because of the low values of μ_{rc} and K for the Amidon material #2 material, the core resistance R_c is much lower than the winding resistance R_w. As a result, the overall inductor resistance is $R_{ac} \approx R_w$.

III. Inductor Design Criteria

According to the Amidon core data sheet, the number of turns to be wound on the core is given by

$$N = 100\sqrt{\frac{L}{A_L}} \tag{18}$$

where the inductance L is in μH and A_L (μH/100 turns) is the inductance factor (A_L = 84 μH/100 turns for a Amidon T94 material #2 core). As a result, 95 turns should be wound on this core to achieve an inductance of 75 μH.

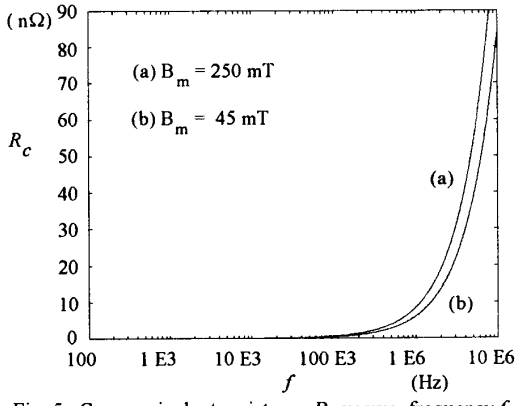

Fig. 5. Core equivalent resistance R_c versus frequency f.

The number of turns that can be wound on one layer is calculated as follows:

$$N_{TL} = \frac{\pi d_i}{t} \tag{19}$$

where d_i (mm) is the internal diameter of the ring core. To reduce the parasitic capacitance, increase the first self-resonant frequency, and achieve the lowest ac resistance, only one layer should be wound on the core. Since the internal diameter of a T94 toroidal core is d_i = 14.3 mm, (19) yields a maximum external diameter of the solid round wire t = 0.47 mm. The available wire with an external diameter close to t = 0.47 mm is the AWG#25 with t = 0.51 mm. An AWG#26 solid round wire (with t = 0.46) could be used but it results in a dc resistance 26% higher than the

AVG#25 round solid wire.

Typical design current densities J range from 1 to 5 A/mm^2. Once the rms value of the current I_{rms} and the diameter d of a solid round wire are known, the operating current density is calculated by using $J = 4\, I_{rms} / \pi d^2$.

If a solid round wire with an external diameter $t = 0.51$ mm is used, the number of turns wound on one layer is $N_{TL} = 88$. Since $N = 95$, only 7 turns must be wound on the second layer and the number of layers can be assumed to be $N_\ell = 1$. The dc and winding ac resistance can now be calculated by using (6) and (7). From (17), the core resistance is also calculated.

IV. Experimental Results

The measurements were performed with an HP 4192/A LCR meter for an inductor with a nominal inductance $L = 75$ μH, designed according to the procedure given in the previous section and assembled by winding one layer of 95 turns of a solid round wire with $d = 0.45$ mm on an Amidon toroidal core of iron-powder core material #2. Fig. 7 shows a plot of measured X_s versus frequency. From Fig. 6, it was found that $f_r = 6.2$ MHz and $L_s = L = X_s/\omega = 75$ μH. Hence, from (2), $C = 8.78$ pF. The dc resistance calculated from (6) is $R_{dc} = 0.28\ \Omega$. This was also the measured inductor resistance at $f = 5$ Hz, that is, the lowest operating frequency of the HP 4192/A LCR meter.

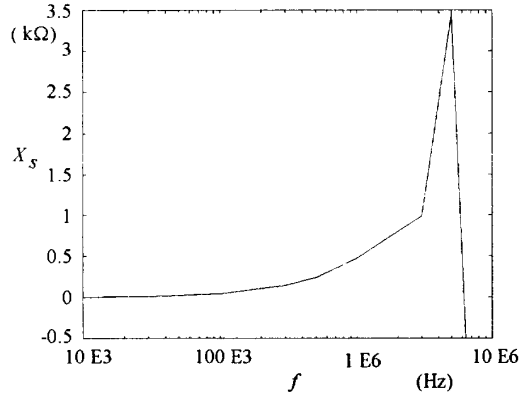

Fig. 6. Measured reactance X_s versus frequency f.

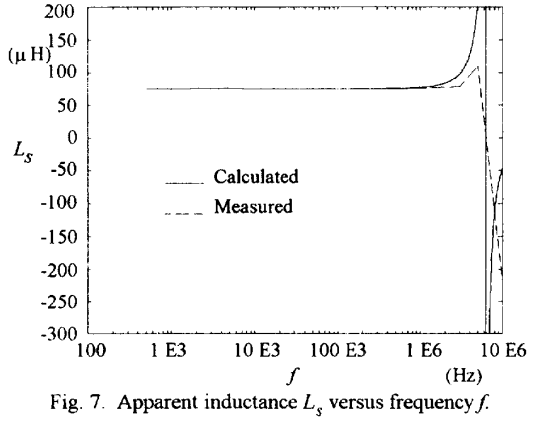

Fig. 7. Apparent inductance L_s versus frequency f.

The measured and theoretical values of the equivalent series inductance L_s are compared in Fig. 8. Both calculated and measured L_s were zero at $f = 6.2$ MHz.

The experimental and theoretical plots of R_s are compared in Fig. 8(a). Note that R_s is approximately ten times higher than R_{dc} at $f = 2$ MHz and R_s increases at higher frequencies. Reactance X_s is depicted in Fig. 8(b). The calculated and measured values of both R_s and X_s are practically the same for $f < f_r$. Note that around the self-resonant frequency accurate measurements cannot be achieved with an LCR meter because the meter can only be operated at factory specified frequencies.

Fig. 9 shows that the impedance magnitude and phase of the equivalent circuits of Fig. 2 closely agree with those of the real inductor. Phase ϕ increased with frequency starting from 0 °C because both real inductor and equivalent circuit behave as a resistor when driven by a dc current and/or voltage.

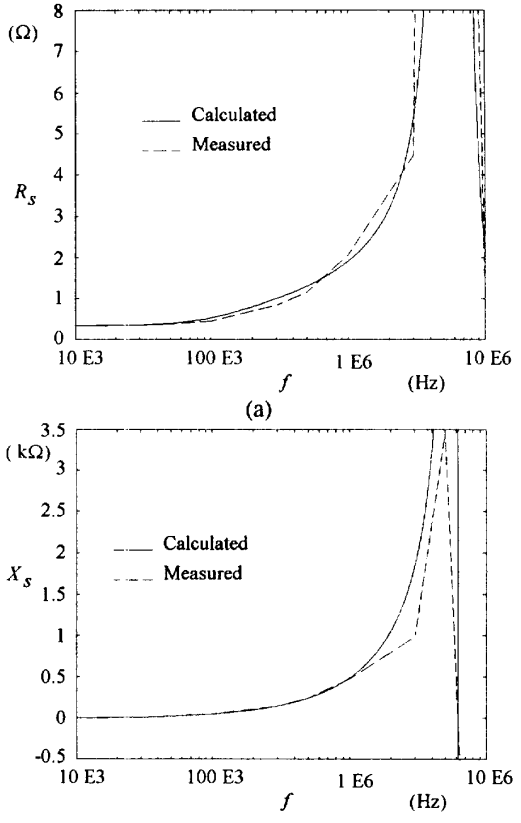

Fig. 8. Inductor impedance Z_s versus frequency f.
(a) Series resistance R_s versus frequency f.
(b) Series reactance X_s versus frequency f.

The plots of the calculated and measured quality factor of the inductor are shown in Fig. 10. The maximum measured value of Q_s was 228 and occurred at $f = 1$ MHz. The theoretical values were in good agreement with those experimentally measured up to about 60 % of the

self–resonant frequency f_r.

The plot of Q_o given by (5) is compared with the plot of measured Q_s in Fig. 11. The values of Q_o are nearly equal to the measured ones for frequencies up to f = 500 kHz.

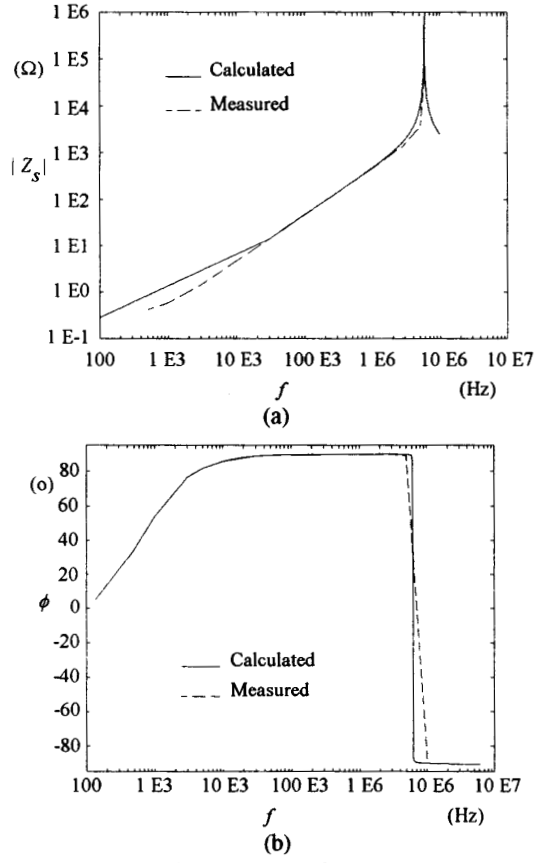

Fig. 9. Inductor impedance Z_s versus frequency f.
(a) Magnitude | Z_s | versus frequency f.
(b) Phase f versus frequency f.

The comparison of the plots of R_s and R_{ac} depicted in Fig. 12 demonstrates that the effect of parasitic capacitance C is negligible up to 1 MHz, that is, up to 20 % of the self resonant frequency. Therefore, for frequencies lower than 1 MHz, the equivalent series resistance of the inductor can be predicted by using the presented equivalent circuit and using the core and wire data sheets. Since the expressions for R_{ac} and Q_o do not require the self–resonant frequency and parasitic capacitance to be known, they can be predicted without the need of any measurement. Therefore, they can be used when designing the inductor. Inductor temperature rise is one important parameter which should be controlled during the inductor design. From Amidon core data sheet, the temperature rise is given by

$$\Delta T_{20^o} = \left(\frac{P_I}{S_a}\right)^{.833} = \left\{\frac{0.5R_{ac}I_m x10^3}{\pi\left[hd_o + hd_i + 0.5\left(d_o^2 - d_i^2\right)\right]}\right\}^{.833} \qquad (20)$$

where P_I is the overall power loss in the inductor in mW and S_a is the surface area of the toroidal core in cm^2, h is the core height in cm, d_i is the inner diameter of the core in cm and d_o is outer diameter of the core in cm. From the wire data sheets, it is found that the copper resistance per unit length at T = 100 °C is 33% higher than at T = 20 °C.

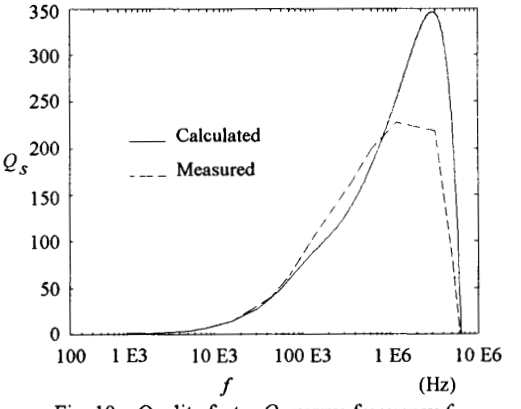

Fig. 10. Quality factor Q_s versus frequency f.

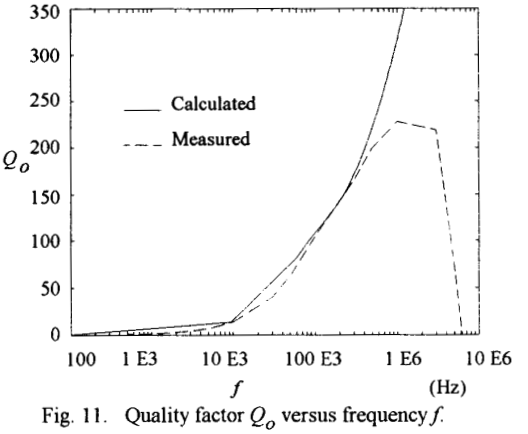

Fig. 11. Quality factor Q_o versus frequency f.

Assuming that the resistance per unit length of the copper is proportional to the operating temperature, the ac resistance R_{ac} as a function of the operating temperature is given by

$$\begin{aligned} R_{ac}(T) &= (1 + 4.125x10^{-3}\Delta T_{20^o})R_{ac}(20^o) \\ &= (912.5x10^{-3} + 4.125x10^{-3}T)R_{ac}(20^o) \end{aligned} \qquad (21)$$

where ΔT_{20^o} is the temperature rise with respect to a 20 °C ambient temperature. Substitution of (21) into (20) allows the operating temperature of the inductor to be calculated. For a T94 toroidal core, the surface area is S_a = 15.31 cm^2. If the core is operated at f = 330 kHz, then the ac resistance at 20 °C is R_{ac} = 0.86 Ω. Assuming a sinusoidal current through the winding with an amplitude of I_m = 1.5 A a power loss P_I = 0.95 W is calculated at T = 20 °C, the temperature rise is ΔT_{20^o} = 35 °C, the operating temperature

°C, the operating temperature of the inductor is $T = 55$ °C, the ac resistance at this temperature is $R_{ac} = 0.97\ \Omega$, and the effective power loss is $P_l = 1$ W at $T = 55$ °C.

A solid round wire with a larger diameter can be used to achieve a lower dc resistance. If 95 turns of a solid round wire with $d = 0.9$ mm, $t = 0.99$ mm, and $r_L = 262.6x10^{-6}$ Ω/mm are wound on a T94 toroidal core, a dc resistance $R_{dc} = 0.069\ \Omega$ is achieved. As expected, this resistance is four times lower than the dc resistance of the winding assembled with a 0.45 mm diameter round wire. As shown in Fig. 13, if the coil has one layer only, also the ac resistance R_{ac} is lower over the entire frequency range. However, from (19), the number of turns that can be wound on one layer is $N_{TL} = 45$ and, therefore, two layers are needed to achieve an inductance $L = 75$ μH. Fig. 13 shows that the ac resistance for the winding assembled with two layers of $d = 0.9$ mm is higher than the ac resistance of the winding assembled with a single layer of $d = 0.45$ mm round wire for $f > 30$ kHz.

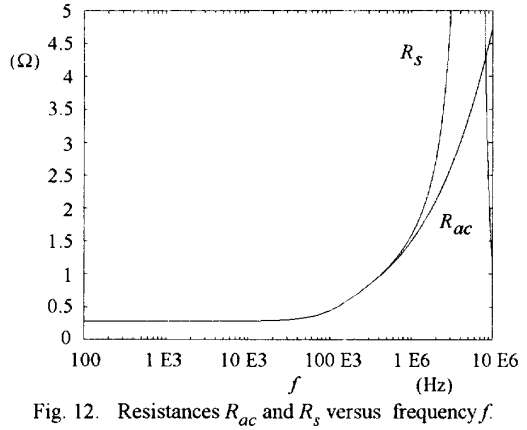

Fig. 12. Resistances R_{ac} and R_s versus frequency f.

V. Conclusions

An equivalent circuit of an iron–powder core inductor including parasitic capacitances and resistances has been examined. The winding ac resistance due to the skin and proximity effects have been considered. The expression for the impedance of the inductor model has been derived along with the procedure for identifying the equivalent circuit components. Experimental and theoretical plots of parameters such as the magnitude and phase of the impedance, the equivalent series resistance, the equivalent series reactance and inductance, and the quality factor have been plotted versus inductor operating frequency and compared. The theoretical values match all of the measured parameters for an operating frequency below the first self–resonant frequency of the inductor. Above the self–resonant frequency, both the equivalent circuit and tested inductor behave as a capacitor. It has also been demonstrated that the quality factor of an inductor highly depends on the operating frequency. The inductor can be modeled by a series combination of an inductance and a resistance for operating frequencies up to 20 % of f_r, while beyond this frequency capacitor C should be taken into account. Core loss is much lower than copper loss also at high flux densities. Moreover, the core resistance is not significantly affected by flux density variations. For these reasons, the overall inductor resistance is primarily determined by the winding resistance.

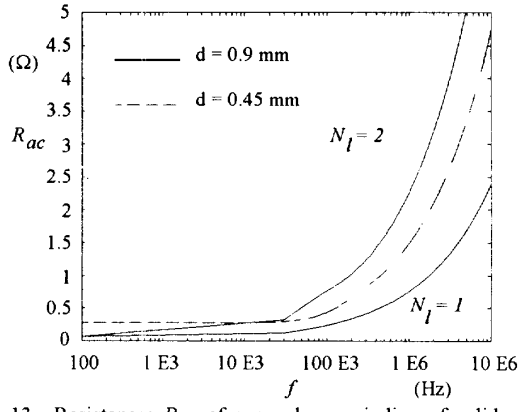

Fig. 13. Resistances R_{ac} of a one layer winding of solid round wire with $d = 0.45$ mm and one layer and two layer winding of solid round wire with $d = 0.9$ mm versus frequency f.

The inductor equivalent series resistance and associated power losses can be calculated for an operating temperature higher than 20 °C by using appropriate values of ρ, r_L, and K. Coefficient K should be given as a function of the inductor operating temperature by core manufacturers to allow the designer for an accurate prediction of inductor power loss.

The iron–powder inductor ac resistance highly increases with the operating frequency and also highly depends on the wound number of layers because of the proximity and skin effects on the winding. As a consequence, the dc resistance is reduced if the solid wire diameter is increased. However, this results in a higher ac resistance when the number of the winding layers is increased.

It has been shown that the lowest ac resistance is achieved when only one layer is wound on the core, if a solid round wire is used. Further studies are recommended for strand and Litz wires.

Approximated expressions of single layer and multilayer equivalent series winding resistances have been introduced. This allows for an immediate evaluation of the high frequency resistance of the winding during the inductor design. The frequency range where the winding resistance does not significatively differs from the dc resistance has been also determined.

The examined equivalent circuit can also be used for inductor operated at non sinusoidal current waveforms. In this case, the equations given in this paper have to be evaluated for a sufficiently large number of harmonics of the inductor current.

The inductor model along with the procedure for extracting the values of the parasitic components can be used by designers to determine the frequency range an iron–

powder core inductor can properly work and prevent its operation close to the self-resonant frequency and/or with too high values of the parasitic resistance. Moreover, the inductor model can be used in computer simulations of electronic circuits to predict their high-frequency operation.

APPENDIX

The winding ac resistance is

$$R_w = R_{dc}A\left[F_{r1} + \frac{2\left(N_\ell^2 - 1\right)}{3}F_{r2}\right] = R_{dc}F_r \qquad (22)$$

where

$$F_{r1} = \frac{e^{2A} - e^{-2A} + 2\sin 2A}{e^{2A} + e^{-2A} - 2\cos 2A} \qquad (23)$$

$$F_{r2} = \frac{e^{A} - e^{-A} - 2\sin A}{e^{A} + e^{-A} + 2\cos A} \qquad (24)$$

and

$$F_r = A\left[F_{r1} + \frac{2\left(N_\ell^2 - 1\right)}{3}F_{r2}\right]. \qquad (25)$$

Fig. 14 clearly shows that F_{r1} and F_{r2} are nearly constant and approach unity for $A \geq 1$ and $A \geq 4$, respectively. If both $F_{r1} = 1$ and $F_{r2} = 1$, (25) gives (10).

Since in one layer winding only F_{r1} contributes to the winding ac resistance rise with frequency, approximation (10) is applicable for $A \geq 1$, that is, for frequencies higher than f_{bs} given by (11). For a multilayer winding, the F_{r2} represents the major contribution to F_r. Therefore, approximation (10) is accurate for $A \geq 4$, which yields (12).

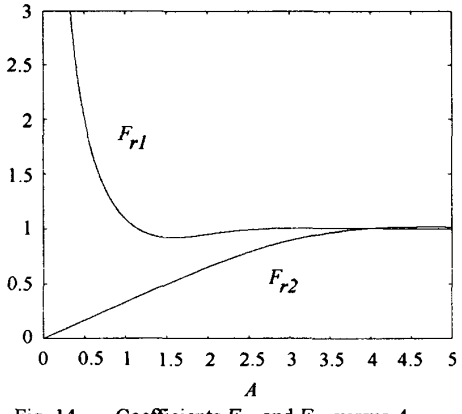

Fig. 14. Coefficients F_{r1} and F_{r2} versus A.

Fig 15 shows that the ratio of the ac and the dc resistance F_r of a one layer winding slightly increases starting from 1 for $A < 1$. Therefore, $R_{ac} \approx R_{dc}$ for $f < f_{bs}$. For $A \geq 1$, F_r linearly increases with A. Using (10), a one layer winding ac resistance ($N_\ell = 1$) is approximated by

$$R_{ac} \approx \left(\frac{4}{\pi}\right)^{1/4} N l_T \left(\frac{\rho \mu_{rw} \mu \pi f}{dt}\right)^{1/2} \qquad \text{for } f < f_{bs}. \qquad (26)$$

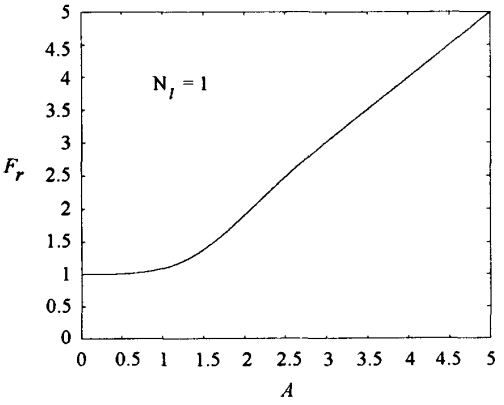

Fig. 15. Coefficient F_r of a one layer winding versus A.

REFERENCES

[1] P. L. Dowell, *"Effects of eddy current in transformer windings"*, Proc. IEE, Vol. 113, No. 8, August 1966, pp. 1287-1394.

[2] C. Wm. T. Mc. Lymann, *"Transformer and Inductor Design Handbook"*, New York: Marcel Decker Inc., 1978.

[3] Colonel Wm. T. Mc. Lymann, *"Magnetic Core Selection for Transformers and Inductors"*, New York: Marcel Decker d Inc., 1982.

[4] W. J. Moore and P. N. Miljanic, *"The Current Comparator"*, United Kingdom: Peter Peregrinus Ltd., 1988.

[5] O. Kiltie, *"Design Shortcuts and Procedures for Electronic Power Transformers and Inductors"*, Cleveland,: Harris Publishing Company, 1975.

[6] W. M. Flanagan, *"Handbook of Transformer Applications"*, New York: Mc. Graw Hill, 1986.

[7] N. R. Grossner, *"Transformers for Electronic Circuits"*, Second Edition, New York: Mc. Graw Hill, 1983.

[8] R. Lee, L. Wilson, and C. E. Carter, *"Electronic Transformers and Circuits"*, Third Edition, New York: John Wiley and Sons, 1988.

[9] M. K. Jutty, V. Swaminathan, and M. K. Kazimierczuk, *"Frequency Characteristics of Ferrite Core Inductors"*, Proc. of *the Electrical Manufacturing & Coil Winding Symposium '93*, Chicago, IL, 1993, pp 369-372.

[10] J. R. Fluke, *"Controlling Conducted Emission by Design"*, New York: Van Nostrand Rehinold, 1991.

[11] K. H. Billings , *"Switchmode Power Supply Handbook"*, New York: Mc. Graw Hill, 1989.

[12] Hewlett-Packard Co., *LCR Meter Model 4192/A Operating Manual.*

[13] J. Jongsma, *"High Frequency Ferrite Power Transformer and Choke Design" - Part 3 "Transformer Winding Design"*, Philips Technical Publication 207, Ordering code: 939805330011.